

# Quantum Wire with Strong Rashba Spin-Orbit Coupling

M. Governale and U. Zülicke

*Institut für Theoretische Festkörperphysik, Universität Karlsruhe, D-76128 Karlsruhe, Germany*

(Dated: October 25, 2019)

We present analytical and numerical results for the effect of Rashba spin-orbit coupling on band structure, transport, and interaction effects in quantum wires when the spin precession length is comparable to the wire width. In contrast to the weak-coupling case, no common spin-quantization axis can be defined for eigenstates within a single-electron band. The situation with only the lowest spin-split subbands occupied is particularly interesting because electrons close to Fermi points of the same chirality can have approximately parallel spins. We discuss consequences for spin-dependent transport and effective Tomonaga-Luttinger descriptions of interactions in the quantum wire.

PACS numbers: 71.10.Pm, 72.10.-d, 73.23.-b

Spin-dependent transport phenomena are currently attracting a lot of interest because of their potential for future electronic device applications[1]. Basic design proposals for spin-controlled field-effect switches[2, 3] use the fact that electron waves with opposite spin acquire different phase factors during their propagation in the presence of Rashba spin-orbit coupling[4] (RSOC). The latter arises due to structural inversion asymmetry in quantum heterostructures[5, 6] where two-dimensional (2D) electron systems are realized. The single-electron Hamiltonian is then of the form[7]  $H_{2D} = H_0 + H_{so}$  where

$$H_0 = \frac{1}{2m} (p_x^2 + p_y^2) \quad , \quad (1a)$$

$$H_{so} = \frac{\hbar k_{so}}{m} (\sigma_x p_y - \sigma_y p_x) \quad . \quad (1b)$$

Possibility to tune the strength of RSOC, measured here in terms of the characteristic wave vector  $k_{so}$ , by external gate voltages has been demonstrated experimentally[8, 9, 10]. As a manifestation of broken spin-rotational invariance, eigenstates of  $H_{2D}$  which are labeled by a 2D wave vector  $\vec{k}$  have their spin pointing in the direction perpendicular to  $\vec{k}$ . Hence, no common spin quantization axis can be defined for eigenstates when spin-orbit coupling is present. Confining the 2D electrons further to form a quantum wire, one might naively expect to again be able to define a global spin quantization axis, as the propagation direction of electrons in a one-dimensional (1D) system is fixed. However, this turns out to be correct only for a truly 1D electron system with vanishing width. In real quantum wires, such a situation is approximately realized when the spin-precession length[2]  $\pi/k_{so}$  is much larger than wire width. Another way to formulate this condition is to say that the characteristic energy scale  $\Delta_{so} = \hbar^2 k_{so}^2 / 2m$  for RSOC is small compared to the energy spacing of 1D subbands. For a quantum wire defined by a parabolic confining potential, e.g.,

$$V(x) = \frac{m}{2} \omega^2 x^2 \quad , \quad (2)$$

the latter would be  $\hbar\omega$ . When spin-orbit coupling is not small (i.e., when  $\Delta_{so} \sim \hbar\omega$  for the case of parabolic

confinement), hybridization of 1D subbands for opposite spins becomes important, resulting in the deformation of electronic dispersion relations[11]. The effect of this deformation on transport properties has been the subject of recent investigation[11], e.g., with respect to implications for the modulation of spin-polarized conductances as a function of RSOC strength[12] which is the principle of operation for spin-controlled field-effect devices[2, 3].

Here we present results for the detailed spin structure of electron states in a quantum wire, defined by the parabolic confining potential  $V(x)$  given in Eq. (2), with strong RSOC present. Contrary to previous assumptions[13] that have been uncritically adopted in the recent literature[14], we find that electrons with large wave vectors in the lowest spin-split subbands have essentially parallel spin. The spin state that right-moving electrons converge toward is opposite to that for left-movers. This result seems surprising initially but is quite obvious when the effect of spin-orbit coupling on 1D subbands is considered carefully. We are going to give a brief qualitative discussion of this point in the following paragraph, before presenting analytical and numerical results for electronic dispersion curves and spin structure of eigenstates. An interesting texture-like variation of spin density *across* the wire is identified. We then turn to a discussion of transport properties based on the Landauer-Büttiker formalism[15, 16]. We find that spin polarized currents whose possible appearance is suggested by the peculiar spin structure are absent in realistic situations when the wire is coupled to contacts where spin-orbit effects are absent. Finally, we discuss consequences for the effective low-energy description of interacting wires in terms of Tomonaga-Luttinger-type models.

We start by discussing basic features for eigenstates of the Hamiltonian  $H_{1D} = H_{2D} + V(x)$  which are 1D plane waves in the  $y$  coordinate with wave number  $k_y$  but bound in  $x$  direction. At finite  $k_{so}$ , spin degeneracy is preserved only for eigenstates with  $k_y = 0$ ; their energies are the shifted harmonic-oscillator levels  $E_n^{(0)} = \frac{\hbar\omega}{2}(2n + 1) - \Delta_{so}$ . This result is exact. To characterize states with

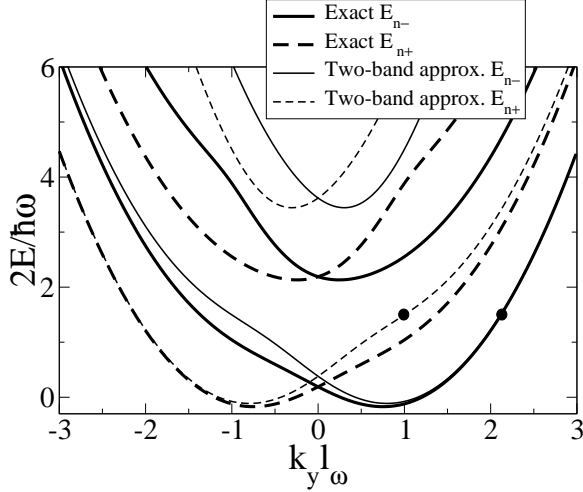


FIG. 1: Lowest and first excited spin-split subbands of a quantum wire, defined by a parabolic confining potential with oscillator length  $l_\omega$  in a 2D electron system, with strong Rashba spin-orbit coupling such that  $k_{\text{so}} l_\omega = 0.9$ . Thick curves are results of the exact numerical calculation, while thin curves are obtained using the approximate two-band model which includes only spin-orbit induced mixing of the lowest two parabolic subbands. Evidently, this approximation gives reasonable results for the lowest spin-split subband, even in the present case of a rather large spin-orbit coupling strength.

finite  $k_y$ , we rewrite  $H_{1D} = H_{\text{pb}} + H_{\text{mix}}$  where

$$H_{\text{pb}} = \frac{p_x^2}{2m} + \frac{m\omega^2 x^2}{2} + \frac{\hbar^2 k_y^2}{2m} + \frac{\hbar^2 k_{\text{so}} k_y}{m} \sigma_x, \quad (3)$$

and  $H_{\text{mix}} = -\hbar k_{\text{so}} \sigma_y p_x / m$ . Straightforward calculation yields eigenstates of  $H_{\text{pb}}$  which are also eigenstates of  $\sigma_x$  with eigenvalue  $\sigma = \pm 1$  and have energies  $E_{n\sigma}^{(\text{pb})}(k_y) = \frac{\hbar\omega}{2}(2n + 1) + \frac{\hbar^2}{2m}(k_y + \sigma k_{\text{so}})^2 - \Delta_{\text{so}}$ . The term  $H_{\text{mix}}$  induces mixing between the shifted parabolic subbands  $E_{n\sigma}^{(\text{pb})}(k_y)$ . To lowest order in perturbation theory, it results in a uniform shift of eigenenergies by  $-\Delta_{\text{so}}$  and a small deviation of spin quantization in  $x$  direction[17]. Hence, for  $\Delta_{\text{so}} \ll \hbar\omega$ , eigenstates of  $H_{1D}$  have energy dispersion  $E_{n\sigma}^{(\text{pb})}(k_y) - \Delta_{\text{so}}$  and are, to a good approximation, eigenstates of  $\sigma_x$ . When  $\Delta_{\text{so}}$  becomes comparable to the subband splitting, however, anticrossings occur between neighboring subbands with *opposite* spin index  $\sigma$ . As a result, no common spin-quantization axis can be defined anymore for eigenstates within any subband. Far enough from anticrossings, however, eigenstates of  $H_{\text{so}}$  will essentially be eigenstates of  $H_{\text{pb}}$ . In particular, their spins will be approximately aligned in  $x$  direction. In the lowest two subbands, right-movers with wave vectors larger than that of the anticrossing point can then have approximately parallel spin. The same is true for left-movers whose asymptotic spin direction is actually opposite to that of right-movers.

In Fig. 1, we show as thick lines numerically calculated

spectra of  $H_{1D}$  for a large value of spin-orbit coupling[25]. Deviation from parabolicity is clearly visible. Interestingly, it is possible to obtain a good quantitative description of the lowest spin-split subband by diagonalizing  $H_{1D}$  in a truncated Hilbert space which is spanned by the lowest and first-excited spin-degenerate parabolic subbands of the Hamiltonian  $H_0 + V(x)$ . We call this the *two-band* model and find an approximate expression for the dispersion of the lowest spin-split subband,

$$\frac{2E_{0\gamma}^{(2b)}}{\hbar\omega} = 2 + (k_y l_\omega)^2 - \sqrt{(1 - \gamma 2k_{\text{so}} k_y l_\omega^2)^2 + 2(k_{\text{so}} l_\omega)^2}, \quad (4)$$

where  $l_\omega = \sqrt{\hbar/m\omega}$  denotes the oscillator length of the parabolic confinement, and  $\gamma = \pm$  is a subband index that does *not* have the meaning of a spin quantization number. We show Eq. (4) and the corresponding result for the first excited subband as thin lines in Fig. 1. There it is seen that the two-band model is quite adequate for the lowest subbands, even for rather strong spin-orbit coupling, but fails for higher ones.

Results shown in Fig. 2 confirm conclusions reached in our previous discussion of the spin structure of electron eigenstates with RSOC present. Panel a) shows the expectation value of spin component in  $x$  direction for eigenstates of  $H_{1D}$  in the lowest and first excited spin-split subbands for the same value of  $k_{\text{so}}$  used in Fig. 1. Data in Figs. 1 and 2 for the same subband are indicated by the same line type. For the lowest subbands, we also give, as thin lines, results obtained analytically within the two-band model. It is clearly seen that spins of eigenstates with large absolute value of wave number are approximately quantized in  $x$  direction, with spin direction of left-movers being opposite to that of right-movers[26]. This fact is underscored by the properties of the energy spectrum in a finite magnetic field  $B$  in  $x$  direction which is shown in panel b). Clearly, Zeeman shift of states at large positive wave number is opposite to that for states with large negative wave number. Shown as thin lines in the main figure of panel a) are curves obtained analytically within the two-band model which yields again reliable results for the lowest subbands. We therefore use it to calculate the variation of spin density  $\vec{s}(x) = \Phi^\dagger(x) \vec{\sigma} \Phi(x)$  across the wire. [The spinor  $\Phi(x)$  denotes the transverse part of an eigenfunction of  $H_{1D}$  which, in the presence of spin-orbit coupling, depends on wave vector.] It turns out that the density  $s_y(x)$  of spin component parallel to the wire vanishes identically. Hence, only the  $x$  and  $z$  components of spin density are shown in Fig. 3, displaying an interesting texture-like variation with coordinate  $x$  whose structure reflects the mixing between subbands due to  $H_{\text{mix}}$ . Note that the expectation value for the  $z$  component of spin, i.e., the one parallel to the growth direction of the semiconductor heterostructure, vanishes for eigenstates of  $H_{1D}$ .

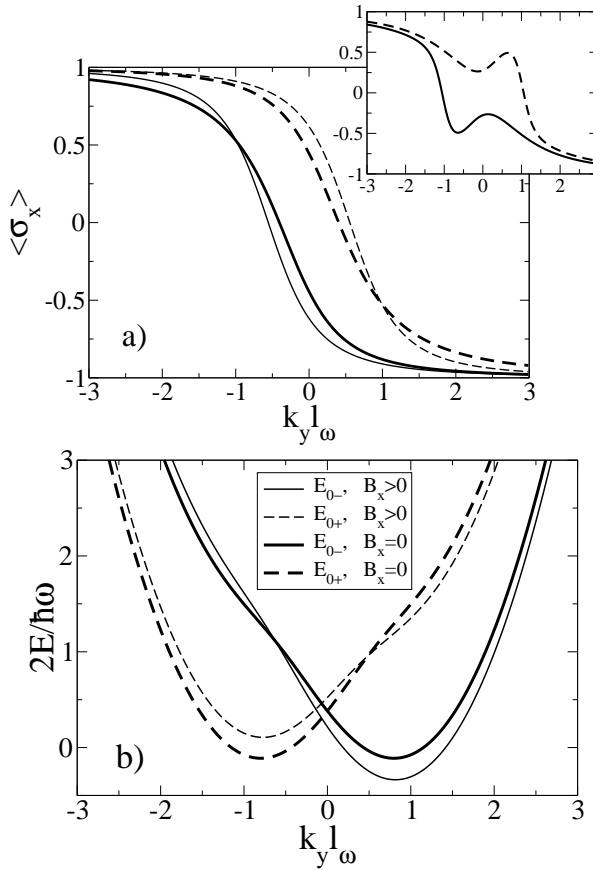


FIG. 2: Spin structure of electron states in a quantum wire with strong Rashba spin-orbit coupling present. Panel a): Expectation value of spin projection onto the  $x$  direction (perpendicular to both the wire axis and the growth direction of the semiconductor heterostructure) for single-electron states obtained in Fig. 1. Results of exact numerical calculation for the lowest spin-split subbands (main figure) and first excited spin-split subbands (inset) are given by thick curves. The effective two-band model reasonably approximates the behavior of the lowest subband (thin lines in the main figure). Right-moving electrons with large wave vectors asymptotically have parallel spin which is opposite to that of left-movers. The same can be observed in panel b) where the spectrum in a finite magnetic field  $B$  pointing in  $x$  direction is compared with that in zero field. We used the two-band model to calculate dispersion curves of the lowest spin-split subbands for finite Zeeman energy  $g\mu_B B = 0.25\hbar\omega$  (thin lines) and in zero magnetic field (thick lines).

Results presented above make it clear that, in general, spin quantum number is *not* an appropriate way to characterize electron states in a quantum wire with strong RSOC. Only states with wave number  $k_y$  far enough from anticrossing points will asymptotically have their spin quantized in  $x$  direction. From considering Figs. 1 and 2, the following special situation can be envisioned which seems to have rather counterintuitive consequences. At low enough electron density such that only states in the lowest spin-split subbands are occupied, states near the

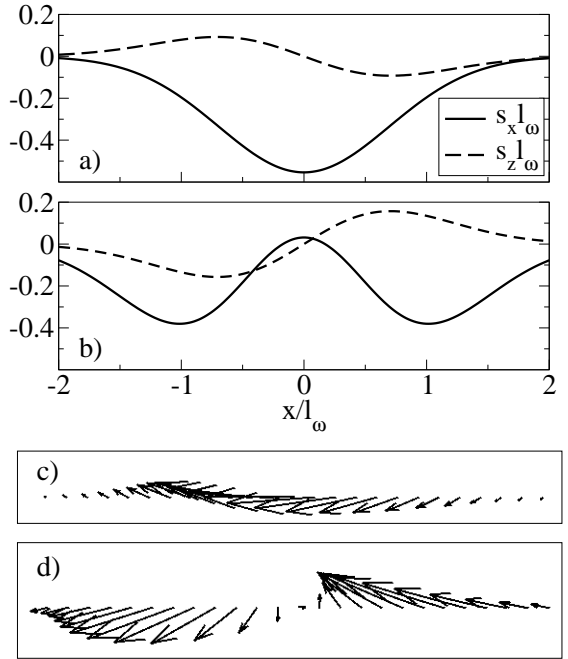


FIG. 3: Texture-like structure of spin density across the quantum wire, calculated within the two-band model for states indicated by black dots in Fig. 1, which have energy  $1.5\hbar\omega$ . a) Spatial variation of nonzero components of spin density for the state with larger wave vector. b) Same for the other state. c) Visualization of spin texture for the same state as a). Arrow length is proportional to spin density. c) Spin texture visualized for the same state as considered in b).

Fermi energy  $\varepsilon_F$  will be localized near four Fermi points. When electron density is not too low, their spins are approximately quantized in  $x$  direction. As pointed out above, spins of states near Fermi points for right-movers are approximately spin-down, opposite to the spin direction of left-moving states near  $\varepsilon_F$ . Assuming it to be possible to selectively raise (lower) the electrochemical potential of right-movers (left-movers), a spin-polarized current could be generated. Usually, creating a population of left-movers and right-movers with different electrochemical potentials is achieved by coupling the quantum wire adiabatically to ideal contacts[15, 16]. However, the underlying assumption that excess electrons injected from the right (left) reservoir will only be spin-up (spin-down) is not realistic because, typically, RSOC will be absent in the contacts. The different nature of electron states in the quantum wire and the leads will result in strong scattering at wire-lead interfaces. Similar to the approach taken in Ref. [12], we model this situation by attaching semi-infinite leads with  $k_{so} = 0$  to the quantum wire where  $k_{so} \neq 0$ . The transmission problem can be solved straightforwardly by matching appropriate *ansätze* for electron wave functions in the wire and the leads. The usual condition for ensuring current conservation has to be modified in the presence of RSOC

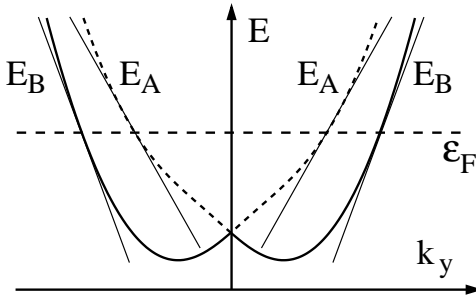


FIG. 4: Schematic depiction of lowest spin-split subbands with linearization around Fermi points. For a low-energy effective description, it is useful to consider right-movers and left-movers having the same velocity as belonging to one particular 1D channel. This simply provides notational convenience and does not reflect any fundamental physical fact.

because the group velocity for electrons in the quantum wire turns out to be an operator in spin space[18, 19]:  $v_y = \hbar(k_y + k_{\text{so}}\sigma_x)/m$ . Despite the unusual spin structure at the four Fermi points which is asymmetric with respect to right-movers and left-movers, no spin-polarized current is generated. This remains true also in the case of a single interface between two semi-infinite wires where  $k_{\text{so}}$  is finite in one half but vanishes in the other half.

Finally, we consider the effective low-energy description of an interacting quantum wire with strong RSOC. In the spirit of Tomonaga-Luttinger models[20, 21] for interacting 1D systems, we linearize the single-electron energy spectrum close to the four Fermi points. See Fig. 4. We explicitly avoid attaching any spin labels. Rather, we define type-A (type B) right-movers and left-movers having velocity  $v_A$  ( $v_B$ ). Typical electron-electron interactions give rise to a term  $H_{\text{int}} = \frac{1}{2} \int_{x',y'} \psi^\dagger \psi(x,y) U(x-x',y-y') \psi^\dagger \psi(x',y')$  in the electron Hamiltonian. In the low-energy, long-wave-length limit, we can write  $\psi(x,y) = \sum_{\alpha=A,B} \sum_{\beta=R,L} \psi_{\alpha\beta}(y) \Phi_{k_F\alpha\beta}(x)$  and assume  $U$  to be long-range on the scale of the wire width but short-range on the scale of the wire length. It is important to note that the present case differs from the usual one in that the transverse wave-function spinors  $\Phi_{k_F\alpha\beta}(x)$  are *nearly orthogonal*. As a result, backscattering processes are strongly suppressed, and only forward-scattering terms need to be kept in the effective low-energy Hamiltonian. Apart from this fact and the peculiar spin structure of states near the four Fermi points, the present system is identical, on a formal level, to a two-component[22] or Zeeman-split[23] Tomonaga-Luttinger model. Response to an external magnetic field will, however, be special in the present case. In particular, with all Fermi points being far enough away from anticrossings, a magnetic field  $B$  applied in  $x$  direction will shift right-movers (left-movers) to higher (lower) energies. [See Fig. 2b).] In the usual bosonization description, the Zeeman term has then the form  $H_Z = -\frac{\Delta z}{2} \int_x \Pi_\rho$ , where  $\Pi_\rho$  is canonically

conjugate to the phase field  $\theta_\rho$  that is related, within the usual[24] phase-field formalism, to the total electron density  $\rho_{\text{tot}} = \sum_{\alpha=A,B} \sum_{\beta=R,L} \rho_{\alpha\beta}$  via  $\partial_y \theta(y) = \rho_{\text{tot}}(y)$ . Approximate orthogonality of transverse parts of electron wave functions enables spin-flip processes, in the long-wave-length limit, only between left-moving and right-moving branches of the same type (A or B). In general, any spin-flip process incurs a large momentum transfer.

This work was supported by the DFG Center for Functional Nanostructures at the University of Karlsruhe.

---

- [1] G. A. Prinz, *Science* **282**, 1660 (1998).
- [2] S. Datta and B. Das, *Appl. Phys. Lett.* **56**, 665 (1990).
- [3] J. Nitta, F. E. Meijer, and H. Takayanagi, *Appl. Phys. Lett.* **75**, 695 (1999).
- [4] E. I. Rashba, *Fiz. Tverd. Tela (Leningrad)* **2**, 1224 (1960), [Sov. Phys. Solid State **2**, 1109 (1960)].
- [5] G. Lommer, F. Malcher, and U. Rössler, *Phys. Rev. Lett.* **60**, 728 (1988).
- [6] R. Winkler, *Phys. Rev. B* **62**, 4245 (2000).
- [7] Y. A. Bychkov and E. I. Rashba, *J. Phys. C* **17**, 6039 (1984).
- [8] J. Nitta, T. Akazaki, H. Takayanagi, and T. Enoki, *Phys. Rev. Lett.* **78**, 1335 (1997).
- [9] T. Schäpers et al., *J. Appl. Phys.* **83**, 4324 (1998).
- [10] D. Grundler, *Phys. Rev. Lett.* **84**, 6074 (2000).
- [11] A. V. Moroz and C. H. W. Barnes, *Phys. Rev. B* **60**, 14272 (1999).
- [12] F. Mireles and G. Kirczenow, *Phys. Rev. B* **64**, 024426 (2001).
- [13] A. V. Moroz, K. V. Samokhin, and C. H. W. Barnes, *Phys. Rev. Lett.* **84**, 4164 (2000).
- [14] A. De Martino and R. Egger, *Europhys. Lett.* **56**, 570 (2001).
- [15] R. Landauer, *IBM J. Res. Dev.* **1**, 223 (1957).
- [16] M. Büttiker, *IBM J. Res. Dev.* **32**, 317 (1988).
- [17] W. Häusler, *Phys. Rev. B* **63**, 121310(R) (2001).
- [18] L. W. Molenkamp, G. Schmidt, and G. E. W. Bauer, *Phys. Rev. B* **64**, 121202(R) (2001).
- [19] U. Zülicke and C. Schroll, *Phys. Rev. Lett.* (2001).
- [20] S. Tomonaga, *Prog. Theor. Phys.* **5**, 544 (1950).
- [21] J. M. Luttinger, *J. Math. Phys.* **4**, 1154 (1963).
- [22] K. Penc and J. Sólyom, *Phys. Rev. B* **47**, 6273 (1993).
- [23] T. Kimura, K. Kuroki, and H. Aoki, *Phys. Rev. B* **53**, 9572 (1996).
- [24] J. Voit, *Rep. Prog. Phys.* **57**, 977 (1994).
- [25] For the purpose of detailed comparison, we have chosen the same value used by Moroz and Barnes [11] in their Fig. 5(c). [Their length  $l_\alpha$  corresponds to  $1/(2k_{\text{so}})$  in our notation.] For some reason unknown to us, their data for eigenenergies at  $k_y = 0$  do not agree with the values  $E_n^{(0)} = \frac{\hbar\omega}{2}(2n+1) - \Delta_{\text{so}}$  which we obtained both from exact analytical calculation and our numerical data. Also, we do not see any hint of nonmonotonicity (“bump”) in the dispersion curves that was elaborated on by Moroz and Barnes [11], e.g., in their Fig. 5(d).
- [26] This result contradicts the spin labeling of subbands adopted in Refs. [13, 14].